Supporting Information

Müller et al. 10.1073/pnas.1304888110

SI Materials and Methods

Generation of CD22 Knockin Mice. ***CD22-R130E.*** The CD22-targeting vector pKS-CD22ex1-5R130E was generated by PCR cloning from 129Sv genomic DNA. The PCR product for the short arm (~1 kb) was amplified and cloned into the pKStkneoLoxP vector by means of introduced NotI and SalI sites with the following primers: 22in5NotAS, 5′-CAC ACT TAA ATG AGC GGC CGC ACT CAC ACT TAA CAT CCA GA-3′ and 22in4SalS, 5′-CGT AGT CGA CGT TGT CGA GGC TCT CAG GTT-3′; restriction sites underlined here and below). The PCR product of the long arm (~4 kb) was amplified and was cloned in by means of introduced ClaI and BamHI sites with the following primers: 22promClaS2, 5′-TCG TAT CGA TTC TGC TCC TGC CTT CGG TGT-3′ and 22in4BamAS, 5′-GCA GGA TCC GGA TTC CAG AAC AGA CAC AA-3′. Point mutations in exon 5 were introduced with the following primers: 9125, 5′-TGG GTC TAG AGA TGA CCG CAG GGA CTG-3′ and 9273, 5′-GTC ATC GCT AGC CCC AGA TTC CCA CTG TCA TTG GC-3′. Standard methods were used to transfect the E14creAG protamine-Cre ES cell line (1) (derived from the 129Sv strain) with the targeting vector. Clones were screened by "semi-nested" PCR (primers: 22in5AS5, 5′-GGT GAC TGA CAG CTA AAC CT-3′ and OlneoE3, 5′-CGC CTT CTA TCG CCT TCT TGA-3′) and Southern blot analysis with an external probe (~450 bp, generated with primers CD22-son-1, 5′-TAA GCC AAT CAG ACC CTA CC-3′ and CD22-son-2, 5′-TCC AAC ACC CTC TTC TGG GC-3′). One positive clone was injected into blastocysts and was transferred into "pseudo- pregnant" females. After germ-line transmission, CD22-R130E mice on a mixed 129Sv/C57Bl/6 background were obtained. Mice carrying the correct mutation in their germ line were identified with PCR and bred to homozygosity. Control mice were age-matched wild-type mice from littermates.

CD22-Y5,6F. The CD22-targeting vector CD22-ITIMko-v2 (with Y2,5,6-F mutations in the CD22 gene) was generated by PCR cloning. The PCR product for the short arm (~1.4 kb) was cloned into the pKStkneoloxP vector by means of introduced SalI and NotI sites with the following primers: 22-in14S-Xho, 5′-ACA CAC TCG AGG GGC ATA TGC CAT AGA GAA-3′ and CD22-in15AS-K-Not, 5′-ACA CAG CGG CCG CAG AGG GTG TGG CTC AGT GGC AGA-3′. The PCR product of the long arm (~6 kb) was cloned in by means of introduced BclI and XhoI-blunt sites with the following primer: 22-in14AS-Bcl, 5′-ACA CAT GAT CAC TAC CGG GTC TTG CAT ATT C-3′. Point mutations in exon 14 and 16 were introduced with the following primers: CD22-13Mut1, 5′-GT**T TT**G CAA TAT TAC GCT TTC CAG AGA GTG-3′ and CD22-13Mut2, 5′-CGT AAT ATT GC**A AA**A CTA ACG GTG TCA TC-3′ [Y2 → F2 mutation (bold)]; CD22-15Mut1, 5′-T**TT C**TC AGA GCT GGT TCA GTT TGG GGC TGG TAA GCG GCC CCA GGC AAA GGA AGA CGT CGA C**TT T**GT GAC CCT CAA GCA CGT A-3′ and CD22-15Mut2, 5′-C**AA A**GT CGA CGT CTT CCT TTG CCT GGG GCC GCT TAC CAG CCC CAA ACT GAA CCA GCT CTG A**GA A**AT GGA TGC TCT-3′ [Y5,6 → F5,6 mutation (bold)]. E14creAG protamine-Cre ES clones were screened by "nested" PCR (primers for first PCR: OlneoE2, 5′-CGG TAT CGC CGC TCC CGA TT-3′ and YFnes5, 5′-GGT GCC TCT AGG GAC TGA TT-3′; primers for second PCR: OlneoE3 (described above) and YFnes7, 5′-CCC TCT AGG CAC CAA GAA GC-3′) and Southern blot analysis with an external probe (~1 kb, generated with primers CD22-son-3, 5′-AGG GGC TTC TAT ACT CTC AAT GA-3′ and CD22-son-4, 5′-GCC TAG ACC CAC AGT TGC TT-3′). One positive clone, which had lost the Y2 mutation was injected into blastocysts (as described above).

CD22-Y2,5,6F. The CD22-targeting vector CD22-ITIMko-v2 was elongated by attaching exons 6 and 7 to the long arm for a better homologous recombination. The following primer pairs were used for the nested PCR: neoneu2, 5′-CCA GCT CAT TCC TCC CAC TCA-3′ and ITIMko ver2_2, 5′-CTG CAC TTG GCT TCT ATT CAG-3′ for the first round and neoneu1, 5′-TGA AGA ACG AGA TCA GCA GCC-3′ and ITIMko ver2_3, 5′-CCT GAG CTA CAG AGT GAG TTG-3′ for the second round. E14creAG protamine-Cre ES clones were screened by nested PCR. Southern blot analysis was performed with an external probe (~1 kb, as described above) and an internal "neo" probe (~650 bp, digested with PstI from plasmid PMCneoPolyA). One positive clone with all present Y–F mutations (Y2,5,6F) was injected into blastocysts (as described above).

Immunizations and ELISA. Mice were immunized intraperitoneally once with Trinitrophenyl (TNP)-Ficoll (10 μg/mouse). Blood samples were taken on indicated days. For Nitrophenyl (NP)-KLH experiments mice were immunized i.p. (100 μg/mouse in alum) three times. The mice were immunized on day 0, day 21, and day 100 and blood samples were taken on indicated days. We measured Ig serum levels by standard ELISA methods. For antigen-specific ELISAs, maxisorp plates (Nunc) were coated with antigen (10 μg/mL TNP-BSA; 5 μg/mL NP-BSA).

1. O'Gorman S, Dagenais NA, Qian M, Marchuk Y (1997) Protamine-Cre recombinase transgenes efficiently recombine target sequences in the male germ line of mice, but not in embryonic stem cell. *Proc Natl Acad Sci USA* 94:14602–14607.

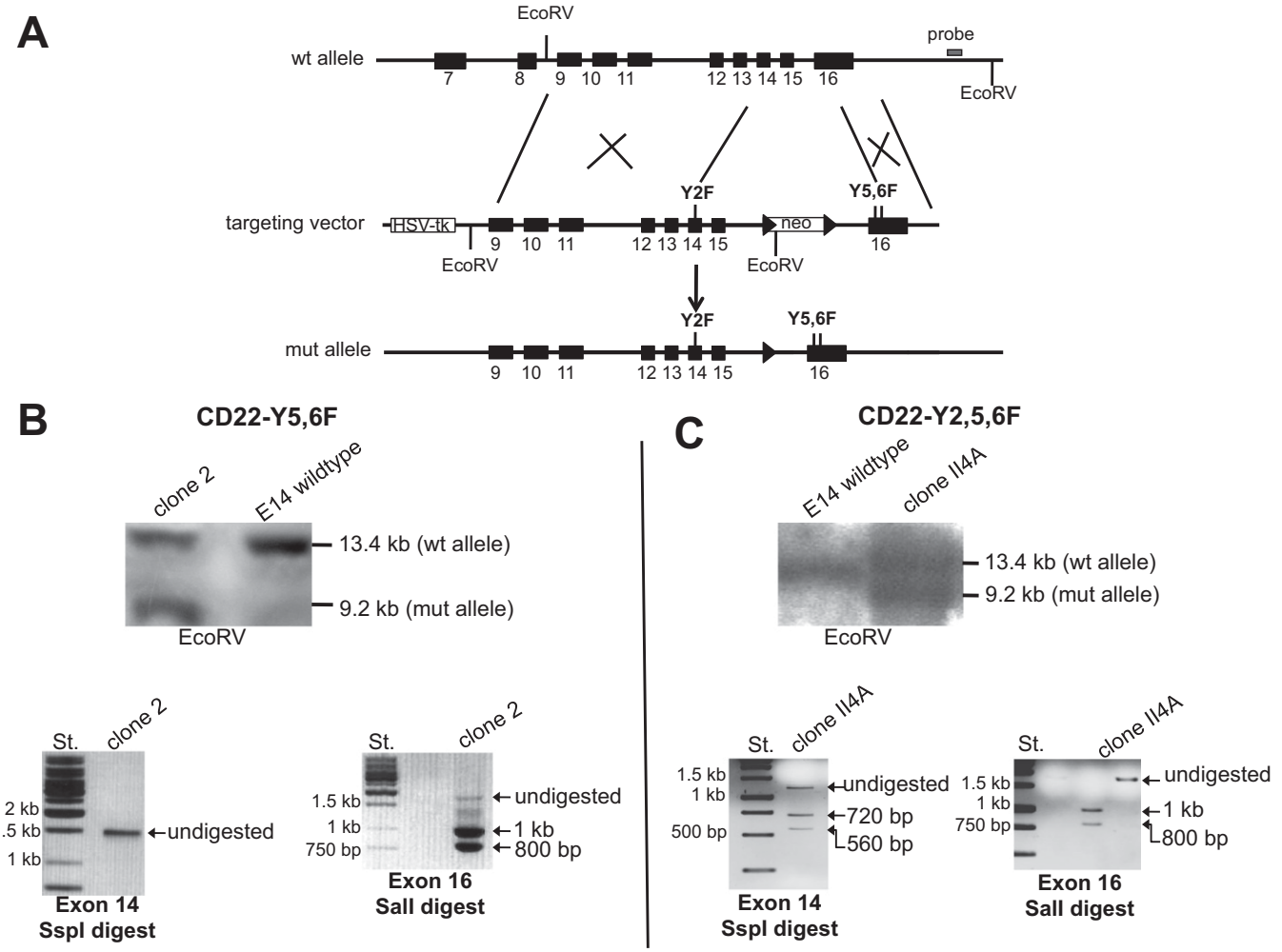

Fig. S1. (*A*) Targeting strategy for generation of CD22-Y2,5,6F mice. Restriction sites and probe for Southern blot are shown. (*B*) ES clone 2 with the Y5,6F mutation is analyzed by Southern blot and by Ssp1 and Sal1 digest (of a PCR amplified fragment) for presence of the introduced restriction sites. The Ssp1 site (Y2F mutation) is lost in this clone. (*C*) ES clone IIA4 with the Y2,5,6F mutation is analyzed by Southern blot and by Ssp1 and Sal1 digest (of a PCR amplified fragment) for presence of the introduced restriction sites. Both sites are present.

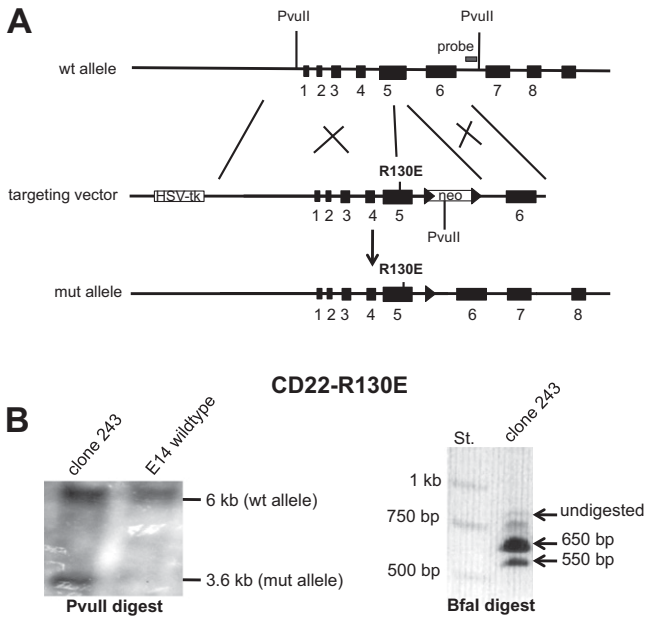

Fig. S2. (*A*) Targeting strategy for generation of CD22-R130E mice. Restriction sites and probe for Southern blot are shown. (*B*) ES clone with the R130E mutation is analyzed by Southern blot and by BfaI digest (of a PCR amplified fragment) for presence of the introduced restriction site.

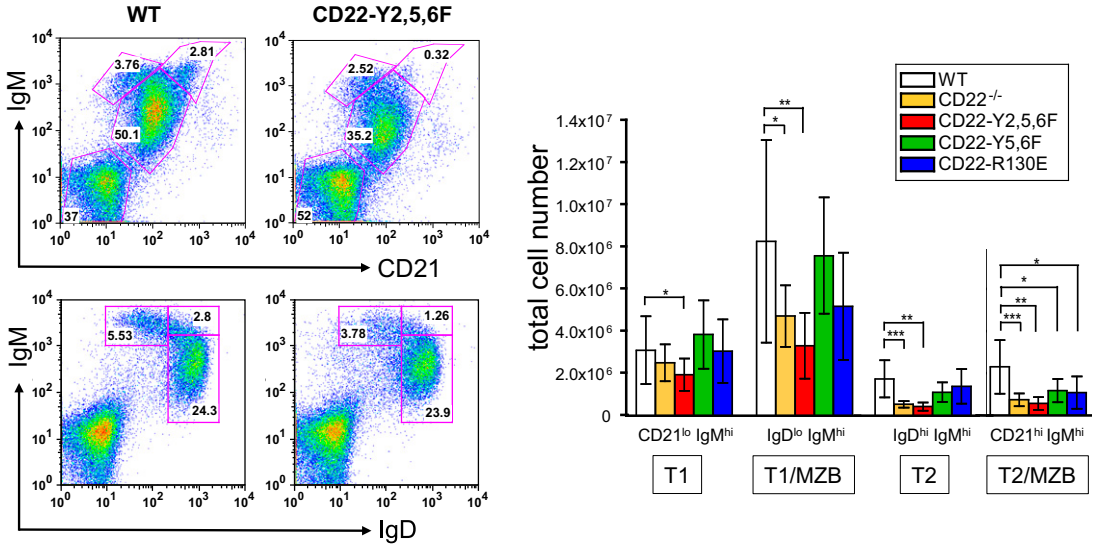

Fig. S3. Transitional B cells are reduced in CD22-Y2,5,6F and CD22$^{-/-}$ mice. Splenic lymphocytes are analyzed by the indicated markers and absolute numbers of transitional (T) and marginal zone (MZ) B cells (T1: CD21^{lo} IgM^{hi}, T1/MZB: IgD^{lo} IgM^{hi}, T2: IgD^{hi} IgM^{hi} or T2/MZB: CD21^{hi} IgM^{hi}) are shown in bar diagrams. *$P < 0.05$; **$P < 0.005$; ***$P < 0.001$. Each experiment was done at least 10–12 times.

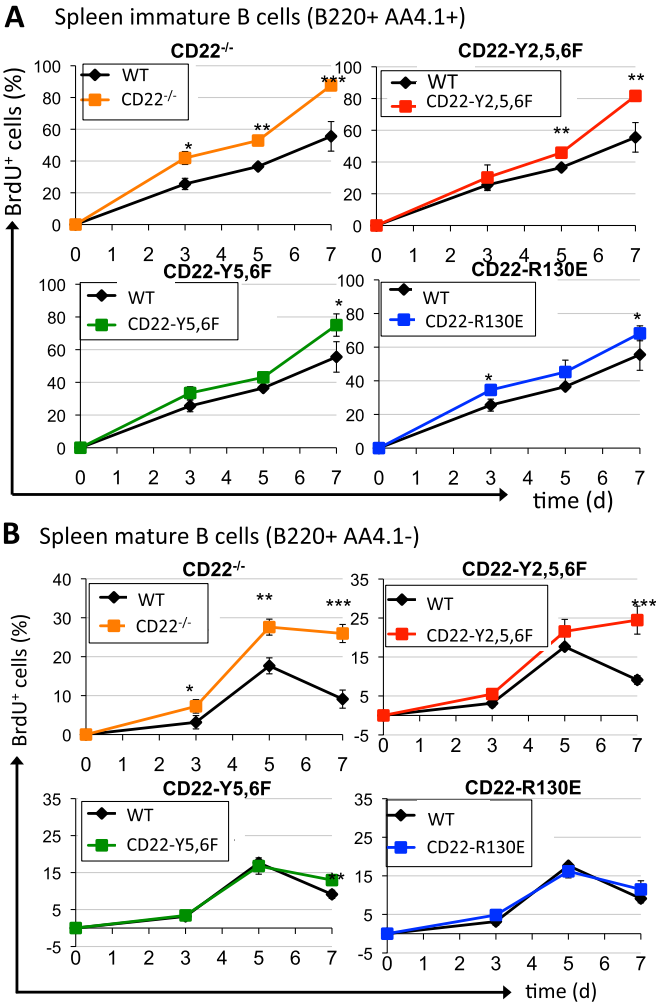

Fig. S4. Higher BrdU incorporation in immature and mature B cells of CD22-Y2,5,6F and CD22$^{-/-}$ mice. (*A*) BrdU incorporation was measured for 7 d in vivo. Immature (B220^{+} AA4.1^{+}) B cells are shown. (*B*) BrdU incorporation was measured for 7 d in vivo. Mature (B220^{+} AA4.1^{-}) B cells are shown. One typical example of two independent experiments is shown. Statistics are summarized results of three mice each. *$P < 0.05$; **$P < 0.01$; ***$P < 0.001$, *P* values are only shown for significant differences.

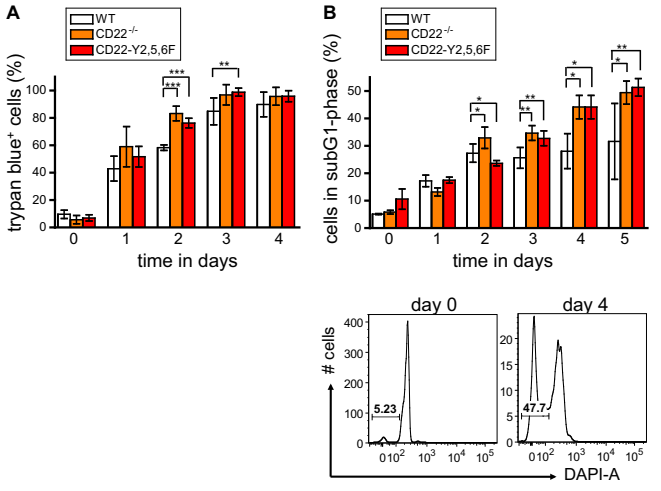

Fig. S5. CD22-Y2,5,6F B cells show a reduced survival rate in vitro. Spontaneous apoptosis rates of splenic B cells of CD22-Y2,5,6F, CD22$^{-/-}$, and control mice in medium without cytokines for indicated time periods measured by (*A*) trypan blue positive cells and (*B*) intracellular DAPI stainings. Apoptosis is determined by events in sub-G1 phase (as indicated *Below*). Data represent typical results of three independent experiments. *$P < 0.05$; **$P < 0.01$; ***$P < 0.001$.

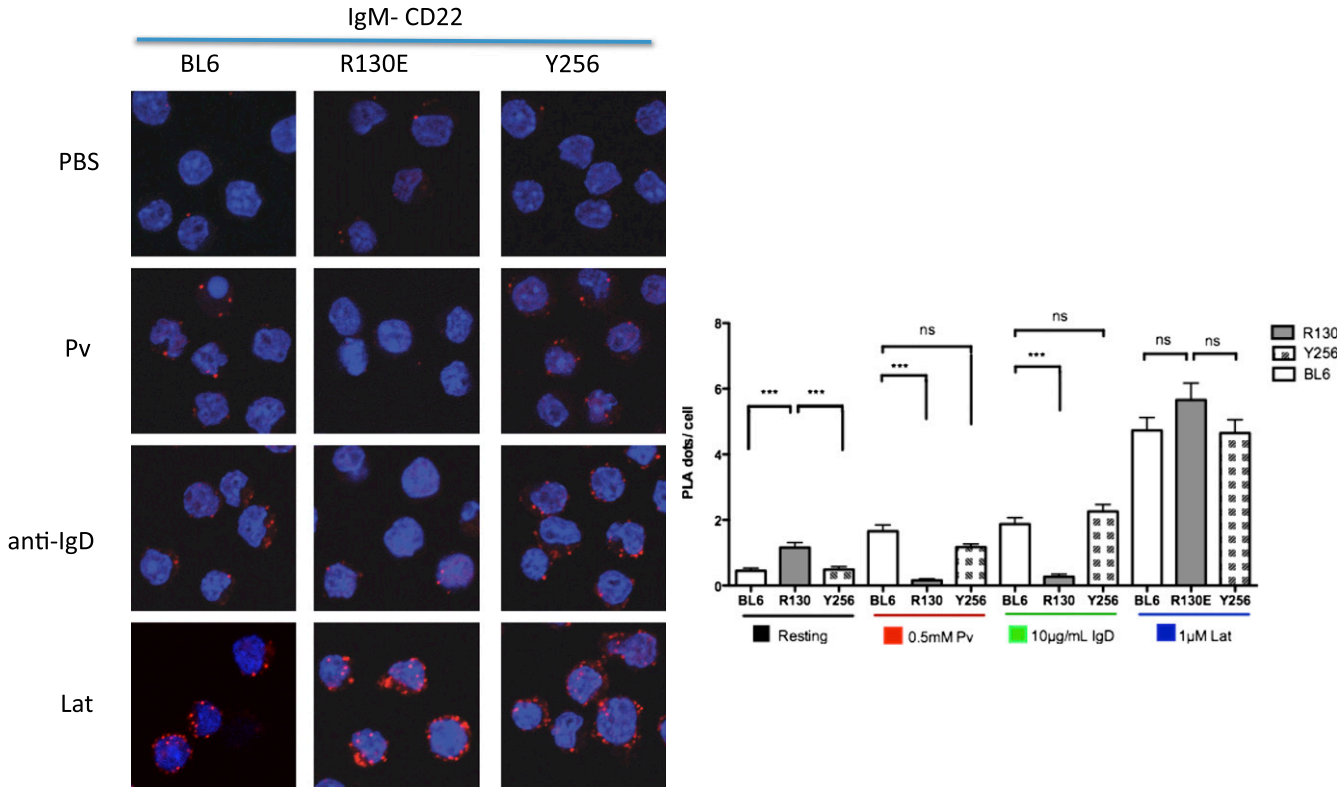

Fig. S6. PLA analysis shows unchanged associations in CD22-Y2,5,6F B cells but changed association of CD22 with IgM in CD22-R130E mice. Association of IgM and CD22 in situ was analyzed by Fab antibodies against CD22 and IgM by proximity ligation assay with B cells of CD22-R130E (R130E), CD22-Y2,5,6F (Y256), or WT control mice. PBS is the unstimulated control, cells were stimulated with pervanadate, anti-IgD or with latrunculin for 5 min. An example is shown on the *Left*, quantitative analysis is shown on the *Right*. One typical experiment out of two is shown.

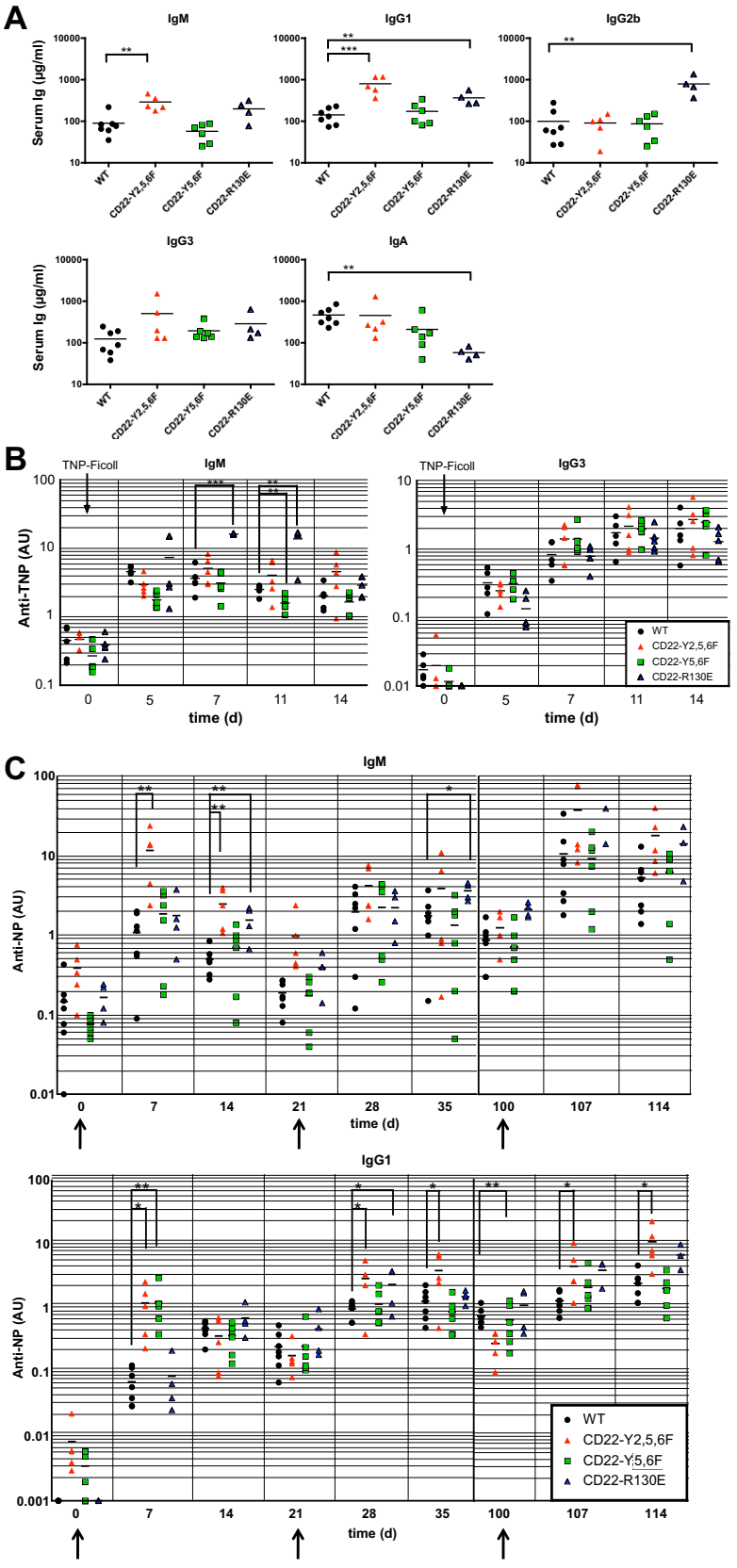

Fig. S7. No major changes in Ig levels and thymus-independent (TI) type 2 responses of CD22 knockin mice, whereas mice with mutated immunoreceptor tyrosine-based inhibition motifs (ITIMs) show higher thymus-dependent (TD) IgG1 reponses. (*A*) Serum Ig levels of the knockin and WT mice were measured by ELISA. (*B*) Mice were immunized with TNP-Ficoll at day 0 and anti-TNP IgM and IgG3 responses were determined by ELISA. One of three independent experiments with similar results is shown. (*C*) Mice were immunized with NP-KLH on day 0, day 21, and day 100 and anti-NP IgM and IgG1 responses were determined by ELISA. One representative experiment out of three independent experiments is shown. Each dot represents one mouse. AU, arbitrary unit. Significances were determined by Student *t* test.

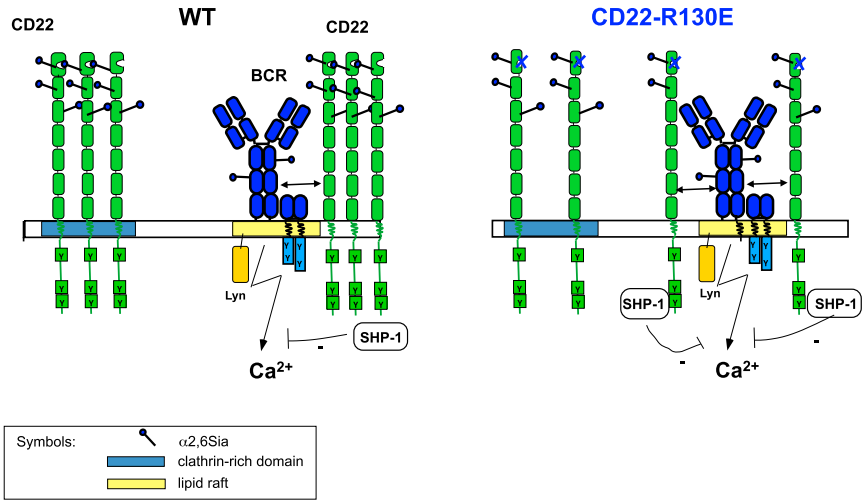

Fig. S8. Model for CD22–B-cell receptor (BCR) *cis*-association. (*Left*) CD22 molecules are bound to a2,6-linked sialic acids of neighboring CD22 molecules, clustered in clathrin-rich domains. After antigen-binding of the BCR, clusters of CD22 are recruited to the BCR. (*Right*) In CD22-R130E mice, the CD22 homooligomeric clusters are disrupted. Consequently a higher association of single CD22 molecules to the BCR can occur upon BCR stimulation. This leads to a higher phosphorylation of CD22 ITIM sequences and a higher signal inhibition.

Table S1. Absolute cell numbers for 10- to 13-wk-old C57BL/6 (control), $CD22^{-/-}$, CD22-Y2,5,6F, CD22-Y5,6F, and CD22-R130E mice (n = 10–12)

Organ/ cell type	WT	$CD22^{-/-}$	CD22-Y2,5,6F	CD22-Y5,6F	CD22-R130E
Bone marrow, $\times 10^5$					
Pro/pre-B cells ($B220^{lo}$ IgM^{neg})	27.9 ± 17	21.6 ± 10.9	16.9 ± 8.1	14.3 ± 10.2	22.6 ± 11.6
Immature cells ($B220^{lo}$ IgM^{med})	11 ± 5.1	8.5 ± 4.0	7.8 ± 4.6	8.9 ± 3.3	9.6 ± 3.6
Transitional B cells ($B220^{lo\text{-}hi}$ IgM^{hi})	4.9 ± 2.1	**2.6 ± 1.2****	**2.9 ± 1.5***	**2.9 ± 1.3***	**3.0 ± 2.0***
Mature B cells ($B220^{hi}$ IgD^{hi})	9.4 ± 3.8	**4.9 ± 2.1****	**4.2 ± 1.3*****	**5.4 ± 2.1****	6.7 ± 2.3
Spleen, $\times 10^6$					
Mature B cells (IgD^{hi} IgM^{med})	16 ± 11	23 ± 9	15 ± 10	17 ± 7	**27 ± 7***
Follicular B cells ($CD21^{lo}$ $CD23^{med}$)	37 ± 19	32 ± 11	23 ± 11	40 ± 13	47 ± 17
Marginal zone B cells ($CD1d^{med}$ $B220^{hi}$)	3.8 ± 1.9	**1.7 ± 0.5****	**1.5 ± 0.7*****	**1.9 ± 0.8***	**1.7 ± 1.0****
T1 B cells ($CD21^{lo}$ IgM^{hi})	3.1 ± 1.6	2.5 ± 0.9	**1.9 ± 0.8***	3.5 ± 1.7	3.1 ± 1.5
T1/MZ B cells (IgD^{lo} IgM^{hi})	8.3 ± 4.8	**4.7 ± 1.5***	**3.3 ± 1.6****	7.0 ± 3.0	5.2 ± 2.6
T2 B cells (IgD^{hi} IgM^{hi})	1.7 ± 0.9	**0.5 ± 0.2****	**0.4 ± 0.2*****	1.0 ± 0.5	1.4 ± 0.8
T2/MZ B cells ($CD21^{hi}$ IgM^{hi})	2.3 ± 1.3	**0.7 ± 0.3****	**0.6 ± 0.3*****	**1.0 ± 0.6***	**1.1 ± 0.8***
MHCII expression on B cells (mfi)	42 ± 17	**81 ± 35***	65 ± 23	77 ± 33	69 ± 27
CD22 expression on B cells (mfi)	597 ± 191	**2 ± 0*****	591 ± 245	606 ± 146	545 ± 119
Peritoneal cavity, $\times 10^5$					
B1a cells ($CD5^{lo}$ $B220^{lo}$)	5.5 ± 3.4	3.1 ± 2.1	5.8 ± 3.7	2.9 ± 2.3	3.2 ± 1.7
B1b/B2 cells ($CD5^{neg}$ $B220^{med}$)	10 ± 4.9	**4.3 ± 2.4****	**4.3 ± 2.6****	**4.3 ± 3.2***	**4.6 ± 1.6****
Lymph node, $\times 10^5$					
Mature B cells (IgD^{hi} IgM^{med})	8.5 ± 4.1	12 ± 6.5	8.3 ± 5.5	15 ± 8.4	**24 ± 11*****
Blood, %					
Mature B cells ($B220^{hi}$ IgD^{hi})	34 ± 10	**19 ± 6*****	**14 ± 7*****	34 ± 12	41 ± 5

Significant changes are emphasized in bold. *$P < 0.05$; **$P < 0.01$; ***$P < 0.001$.